Talanta 83 (2011) 1422–1427

Contents lists available at ScienceDirect

Talanta

journal homepage: www.elsevier.com/locate/talanta

Ultrasensitively sensing acephate using molecular imprinting techniques on a surface plasmon resonance sensor

Chuanping Wei [a], Huiqing Zhou [b], Jie Zhou [a,*]

[a] College of Chemistry and Material Science, Shandong Agricultural University, Taian, Shandong, 271018, PR China
[b] College of Chemistry, Nankai University, Tianjin, 300071, PR China

ARTICLE INFO

Article history:
Received 12 July 2010
Received in revised form
11 November 2010
Accepted 14 November 2010
Available online 19 November 2010

Keywords:
Molecular imprinting
Surface initiated radical polymerization
Surface plasmon resonance sensor
Recovery

ABSTRACT

An ultrathin molecularly imprinted polymer film was anchored on an Au surface for fabricating a surface plasmon resonance sensor sensitive to acephate by a surface-bound photo-radical initiator. The polymerization in the presence of acephate resulted in a molecular-imprinted matrix for the enhanced binding of acephate. Analysis of the SPR wavenumber changes in the presence of different concentrations of acephate gave a calibration curve that included the ultrasensitive detection of acephate by the imprinted sites in the composite, K_{ass} for the association of acephate to the imprinted sites, 7.7×10^{12} M^{-1}. The imprinted ultrathin film revealed impressive selectivity. The selectivity efficiencies for acephate and other structurally related analogues were 1.0 and 0.11–0.37, respectively. Based on a signal to noise ratio of 3, the detection limits were 1.14×10^{-13} M for apple sample and 4.29×10^{-14} M for cole sample. The method showed good recoveries and precision for the apple and cole samples spiked with acephate solution. This suggests that a combination of SPR sensing with MIP film is a promising alternative method for the detection of organophosphate compounds.

1. Introduction

Organophosphorus pesticides (OPPs) are a class of pesticides that generally act as cholinesterase inhibitors and are used for the control of a broad range of pests on cotton, rice, tobacco, sorghum, sugarcane and vegetables. Thus, OPPs have played an important role in increasing agricultural productivity [1]. However, OPPs are highly toxic to all animals and humans, and their residues have always been the most important problem on food security [2,3]. Tolerance levels have been established in many countries of the world. For example, in Europe, a limit value of 0.1 μg/L was set for pesticides in drinking water by the European Community [4]. These limits are set to protect the food supply as well as trade in agricultural products. Therefore, highly sensitive methods for the determination of OPPs in environmental and biological samples are required. Current analytical methods for the detection of OPPs include gas chromatography (GC) [5,6], high performance liquid chromatography (HPLC) [7], gas chromatography–mass spectroscopy (GC–MS) [8] and HPLC–mass spectroscopy [9]. Although several of these methods achieve low levels of detection, in practice they consume large amounts of time and solvent, and require one or more cleanup steps involving liquid–liquid partition or solid-phase extraction [10]. Immunological methods have also been used for the determination of OPPs [11,12]. Nevertheless, these methods are labile to physical and chemical conditions [13]. Since the works reported by Liedberg et al. during the 1980s [14], SPR-based biosensors have been widely developed because, in principle, SPR sensing requires no sample probing [15]. SPR is a versatile tool to probe and detect refractive index changes occurring on metal thin films, e.g., gold films, as a result of chemical events [16,17]. SPR phenomenon occurs during optical illumination of a thin metal film and it is explained as a charge density oscillation. SPR measurements use the optical field enhancement that occurs near the gold surface when surface plasmons are created. The maximum penetration depth of surface plasmons is about 200 nm in the case of aqueous samples at around 9000 cm^{-1}. Within this 100 nm region, the optical fields are sensitive to changes in the index of refraction caused by changes in the thickness of the molecular layer on the gold surface. SPR spectroscopy is thought to be well-suited not only for DNA [18,19] and protein microarrays [20,21], but also for small-molecule microarrays [22–24]. SPR measurements can be made using different methods [25]. One method, the "angle shift" measurement, uses a single wavelength of light for excitation and measures the reflectivity as a function of incident angle. A second method, FT-SPR measurement, is performed at a fixed angle of incident light and reflectivity is measured over a range of wavelengths in the near infrared. Since FT-IR spectrometers typically have high wavenumber resolution, and a wide range of reflection angles are available in an FT-SPR module, FT-SPR is a

* Corresponding author. Tel.: +86 538 8246369; fax: +86 538 8242251.
E-mail address: zhoujie@sdau.edu.cn (J. Zhou).

0039-9140/$ – see front matter © 2010 Elsevier B.V. All rights reserved.
doi:10.1016/j.talanta.2010.11.034

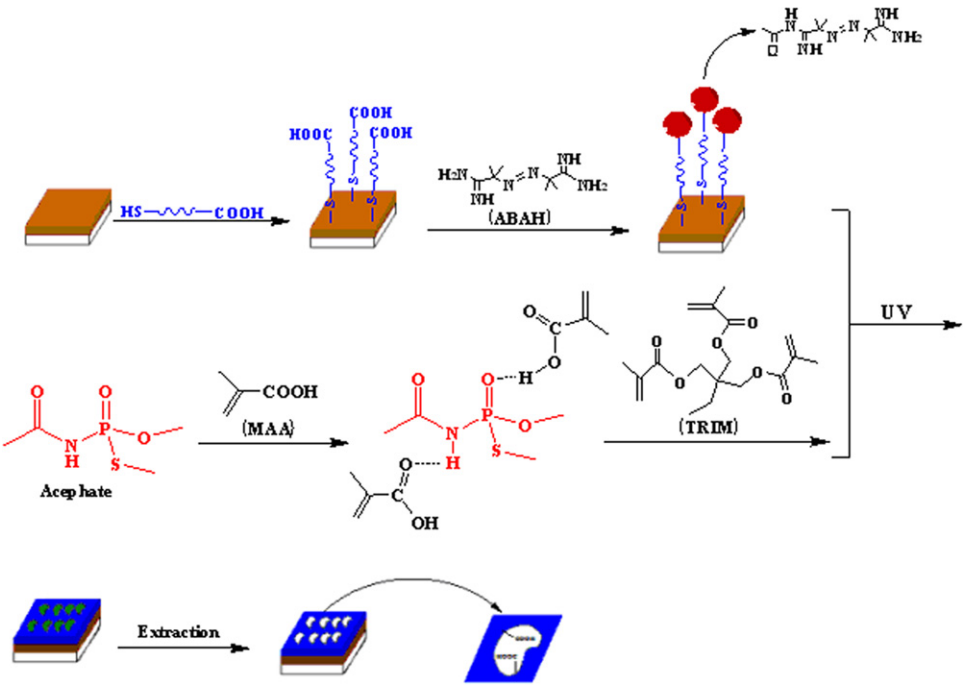

Scheme 1. Illustration of the formation of MIP ultrathin film by a surface-bound photo-radical initiator.

highly sensitive method with remarkable dynamic range for surface analysis.

With SPR, quick measurements can be taken in real time. However, for SPR sensors, chip coatings are usually costly and use unstable receptor molecules, such as antibodies. These limitations have generated the need to investigate potential artificial recognition sites. Among artificial receptors, molecular imprinting polymers (MIPs) have proven their potential as synthetic receptors in numerous applications ranging from liquid chromatography to sensor technology [26,27]. MIPs are extensively crosslinked polymers containing specific recognition sites with predetermined selectivity for analytes of interest. Compared to its biological counterparts, enzymes and antibodies, MIPs can not only display comparable molecular selectivity, but also have chemical inertness, long-term stability, and insolubility in water and most organic solvents [28,29]. In the present work, we prepared an ultrathin MIP film on an SPR sensor chip using surface initiated radical polymerization. The polymer film was directly immobilized on an SPR sensor chip. The imprinting polymerization was carried out in a dilute acetonitrile solution consisting of the template acephate, the functional monomer methacrylic acid, and the crosslinker trimethylolpropane trimethacrylate. Prior to polymerization, a photo-initiator was covalently coupled to a self-assembled monolayer of carboxyl terminated alkanethiol on a gold surface. The imprinted ultrathin film was characterized directly by means of FT-SPR measurements, and showed much higher selectivity toward acephate than structurally correlative OPPs. Furthermore, the performance of the film for the extraction of acephate was evaluated in the analysis of apple and cole samples spiked with acephate.

2. Materials and methods

2.1. Materials

Methacrylic acid (MAA) of analytical grade was purchased from Beijing Chemical Reagent Company (Beijing, China) and distilled before use. Trimethylolpropane trimethacrylate (TRIM,) from Aldrich was extracted with 2 M NaOH solution and water and dried over anhydroxide magnesium sulfate. 11-Mercaptoundecanoic acid (COOH-thiol, 95%), 2-ethyl-5-phenylisoxazolium-3′-sulfonate (NEPIS, 95%), 2,2′-Azobis(2-amidinopropane) hydrochloride (ABAH, 97%) were purchased from Aldrich. Acephate, malathion, phoxim, chlorpyrifos, methamidophos, profenofos and trichlorfor (the purities: >99%) were generously provided by College of Plant Protection Science, Shandong Agricultural University (Taian, China). All solvents (HPLC grade) were from commercial sources and used without further purification. Water was doubly distilled. The gold-sputtered slide glass (18 cm × 18 cm) used as a sensor chip was purchased from Thermo Electron Corp (USA). Acetic acid and sodium acetate (HAc–NaAc) buffer solutions (0.1 M, pH 3.0–8.0) were used in the experiments. All solutions used were filtered using Corning cellulose acetate membranes with 0.45 μm pores.

2.2. In situ preparation of imprinted polymer films

Immobilization of radical initiator on gold surface was carried out using a literature protocol [30]. The gold-sputtered slide glass, as a sensor chip was dipped in 10 mL of freshly prepared piranha solution (70% H_2SO_4, 3% H_2O_2) for 2 min, and rinsed with copious distilled water. It was then placed into 20 mL of 1.0×10^{-3} M solution of 11-mercaptoundecanoic acid in ethanol, and kept at 4 °C overnight. The chip was then rinsed with ethanol and double distilled water. The carboxyl groups on the self-assembled monolayer (SAM) were activated by placing the chip in 10 mL of 1.0×10^{-2} M aqueous solution of 2-ethyl-5-phenylisoxazolium-3′-sulfonate for 30 min. Finally, the chip was then transferred into 10 mL of 0.20 M ABAH aqueous solution and kept at 20 °C for 3 h. The initiator-covered chip was dry under a stream of N_2, and used immediately for polymer preparation. The chip was placed in a solution prepared by dissolving acephate (9.5×10^{-5} mol), MAA (1.1×10^{-3} mol) and TRIM (7.0×10^{-2} mol) in 7 mL of acetonitrile. Prior to polymerization, the prepolymer solution was saturated with N_2 for 10 min. The solution containing the chip was placed in a home-made photochemical reactor and irradiated with UV (350 nm) at 4 °C for 2 h. Thus the surface-grafted imprinted polymer film on a gold-

Table 1
FT-SPR operation parameters.

Parameter	Setting
Sample compartment	Left AEM
Detector	InGaAs
Beam splitter	CaF_2
Source	White light
Recommended range	12400–5400 cm^{-1}
Max range limit	10500 cm^{-1}
Min range limit	6400 cm^{-1}
Velocity	1.2659 mm/min
Aperture	5
Gain	1

sputtered slide glass was prepared. Non-imprinted polymer (NIP) film on an SPR chip was also prepared as described above but without the addition of the template (acephate). When the chip was mounted into the SPR instrument, the chip was washed with 0.5% acetic acid (v/v) in 20% aqueous acetonitrile at a flow rate of 1.2 mL/min until a stable base line was obtained.

2.3. Sample preparation

Samples apple and cole were purchased at a local market in China and homogenized in a food cutter. Two different kinds of synthetic samples were prepared. (1) 10.0 g apple or 20.0 g cole subsamples were put into a 100 mL glass flask and freeze-dried at −80 °C for 24 h, then spiked with acephate standards at 2.00×10^{-11} mol/kg or 5.00×10^{-12} mol/kg and grounded in a mortar containing 0.250 g (or 0.500 g) polyvinylpolypyrrolidone (PVPP) with a pestle until the mixture became homogeneous and left for 1 h. The mixture was placed in a close vial, 20 mL of acetone were added and extracted for 20 min, centrifuged for 15 min at 4 °C, 12000 rpm. Extraction was repeated twice, the combined extracts were evaporated to near dryness in a rotary evaporator at 30 °C. The residue was re-dissolved in 100 mL of HAc–NaAc buffer solution (0.1 M, pH 5.0). The solution was filtered using Corning cellulose acetate membranes with 0.45 μm pores and ultrasonicated for 10 min. (2) 10.0 g apple or 20.0 g cole subsamples were dipped into 30 mL of 1.0×10^{-9} M solution of acephate and kept at 4 °C overnight. The subsamples were transferred into a 100 mL glass flask and freeze-dried at −80 °C for 24 h, then treated with the above-mentioned procedure. For the solution used in the process of leaching, the residual acephate was also determined with the same SPR method.

2.4. FT-SPR experiments

FT–SPR is a label-free detection technique based on the coupling between the incident light and the gold surface plasmon wave. In our experiments, the FT-SPR measurements were performed with an SPR-100 module from Thermo equipped with a flow sample cell mounted on a goniometer. It was inserted in a Thermo Nexus FT-IR spectrometer using a near-IR tungsten–halogen light source. The incidence angle was adjusted to have minimal reflectivity located at 9000 cm^{-1} at the beginning of each experiment so as to be in the best sensitivity region of the Indium Gallium Arsenide (InGaAs) detector. A peristaltic pump was used to pump the analyte or wash solution from a reservoir into the flow cell. HAc–NaAc buffer solution (0.1 M, pH 5.0) was used as a running buffer, and the flow rate was fixed at 1.20 mL/min. Different concentrations of tested compounds dissolved in the running buffer were injected into the flow cell until the wavenumber shifts reached stable values. The stable wavenumber shifts that occurred were recorded in real time using the FT-SPR. In all the experiments, all used solutions were ultrasonicated. Before each binding measurement for the sample solutions, the SPR sensor chips were washed with 0.5% acetic acid (v/v) in 20% aqueous acetonitrile and HAc–NaAc buffer solution (0.1 M, pH 5.0) in turn until a stable base line was obtained. The data (shown as a wavenumber shift in SPR angle) were obtained by

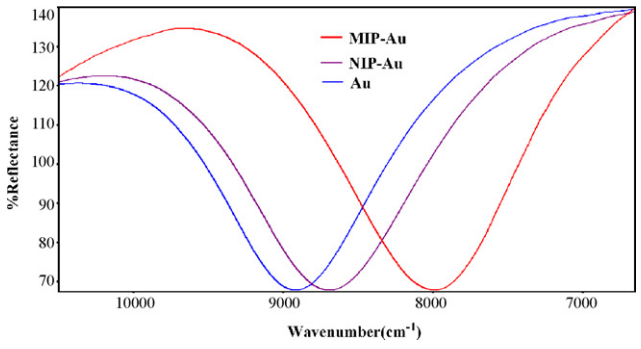

Fig. 1. Typical FT-SPR spectra of the bare, MIP and NIP-modified Au surfaces in 0.1 M HAc–NaAc buffer solution, pH 5.0 at room temperature.

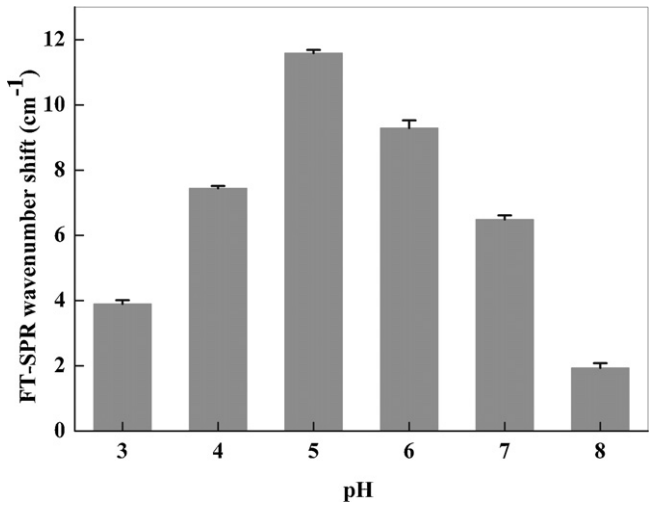

Fig. 2. Effect of pH on the selectivity of Acephate-MIPs ultrathin film. [Acephate] = 6×10^{-12} M.

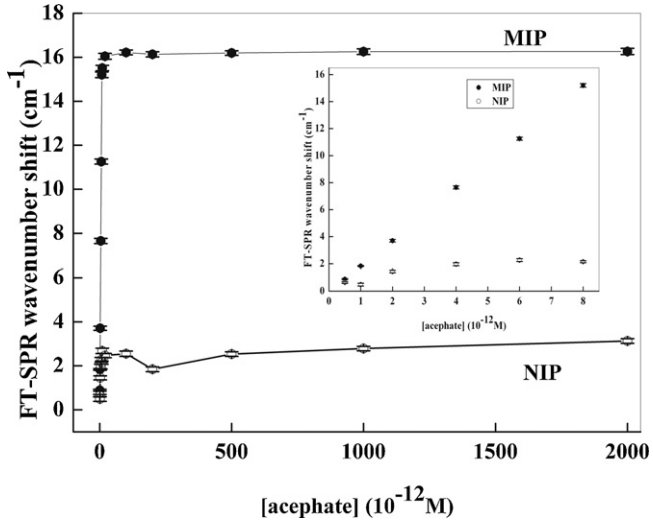

Fig. 3. Changes in the wavenumber shift upon analyzing acephate within a range of concentrations with MIP and NIP ultrathin films. Inset: responses of the MIP and NIP ultrathin films in low concentration range. All measurements were performed in 0.1 M HAc–NaAc buffer solution, pH 5.0.

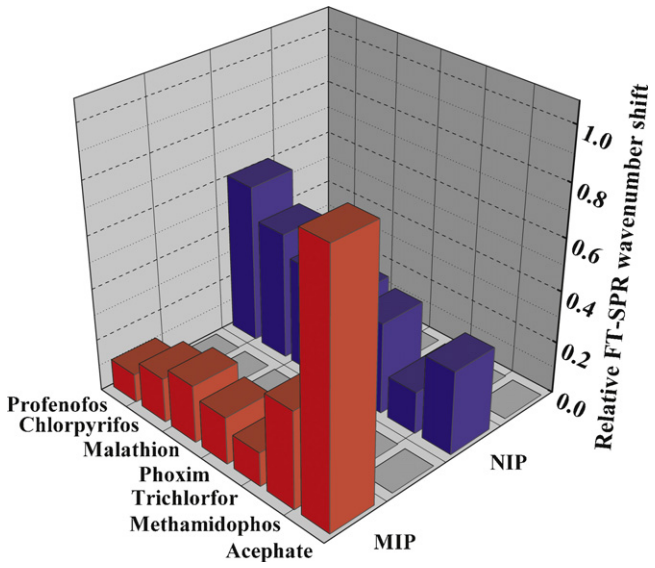

Fig. 4. Selectivity of the MIP and NIP ultratin films. The relative FT-SPR wavenumber shift was calculated by dividing the FT-SPR wavenumber shift for the MIP or NIP film upon injection of each tested OPPs by that for the MIP film upon injection of acephate. Sample concentration was 1.6×10^{-12} M and 5×10^{-9} M for MIP and NIP, respectively. All measurements were performed in 0.1 M HAc–NaAc buffer solution, pH 5.0.

subtracting background data of HAc–NaAc buffer solution (0.1 M, pH 5.0) from those obtained from sample solutions. The average of nine replicated measurements was obtained for each sample at 32 cm^{-1} resolution. Table 1 summarized the operating conditions under which the FT-SPR data were obtained.

3. Results and discussion

3.1. Immobilization and characterization of MIP ultrathin film on an SPR sensor chip

Molecular imprinting was widely employed to in situ assemble an MIP layer directly on transducer surface [31–36]. Lotierzo et al. [36] immobilized a carboxyl functionalized photo-initiator, 4,4′-azo-bis(cyanovaleric acid) on gold chips that were pre-coated with 2-mercaptoethylamine, and used the surface bound initiator to prepare imprinted polymer films for selective detection of domoic acid. Target recognition in water was monitored using an SPR sensor. Piacham et al. [37] immobilized ABAH on a long chain, carboxyl terminated monolayer of alkanethiol on gold surface and prepared a thin (*S*)-propranolol-imprinted film QCM sensor in a well-controlled and reproducible manner. The sensor displayed certain chiral selectivity towards the original template, (*S*)-propranolol at a concentration higher than 3.8×10^{-4} M in aqueous solution. In the present study, with Piacham's approach, the ultrathin acephate-imprinted film on an SPR sensor chip was prepared in a dilute solution of acephate, MAA and TRIM using surface ABAH-initiated radical polymerization (Scheme 1). The use of photo-polymerization at 4 °C was to ensure that the non-covalent adducts between MAA and acephate were efficiently formed in order to increase the imprinting efficiency [38–40].

For quick response, control of the thickness of the imprinted polymer film is important. A thinner is preferable for the analyte molecules diffusing into the ultrathin film to reach the proximity of the gold substrate. The FT-SPR spectra on bare, MIP and NIP-modified Au films in contact with 0.1 M HAc–NaAc buffer solution (pH 5.0) were measured (Fig. 1) at room temperature. Fig. 1 showed that the wavenumber shifts of 928.97 cm^{-1} and 229.43 cm^{-1} at SPR angle 60° were observed onto the MIP and NIP-modified Au surfaces, respectively. This demonstrates that the MIP or NIP-modified film with an adequate deposition thickness was formed by exposing the SPR Au film modified with a monolayer of alkanethiol to a prepolymeric solution. Corn and Weibel report that there exists an optimum angle to perform the SPR wavelength shift measurement [25] and a shift of ca. 4 cm^{-1} at the SPR angle may correspond to approximately 0.1 nm (1 Å) in effective film thickness change of adsorbed layers. Based on the theory, we estimated the thickness of the MIP (NIP) film was about 23 (6) nm. The NIP film was much thinner than the MIP film. This discrepancy might be due to the different action ways of the initiators used in the experiments. For the non-imprinting polymerization, the ABAH initiator used in the present study contains basic functional groups that form strong interaction with the acidic functional monomer (MAA). This would increase local MAA concentration around active radicals. This accelerates incorporation of MAA into the growing polymer chain. The apparent relative reactivity of the crosslinker, TRIM is thus decreased so that no effective crosslinking can be achieved. For the imprinting polymerization (where the basic template acephate is added), the interaction between MAA and the basic initiating radicals is disrupted, therefore ABAH acts as the commonly used non-polar photo-radical initiator, azobis-isobutyronitrile (AIBN). This leads to effective incorporation of TRIM into growing polymer chains and results in surface crosslinked MIP network.

3.2. Effect of pH on the performance of the MIP SPR sensor chip

The effect of pH on the performance of the MIP SPR sensor chip was studied by varying the pH in the range of 3.0–8.0 HAc aqueous solution (0.1 M) was adjusted to different pH with concentrated NaOH solution. The obtained results were shown in Fig. 2. As can be seen from Fig. 2, when the pH increased from 3.0 to 5.0, adsorption of the analyte on the MIP film reached a maximum. However when the pH increased from 5.0 to 8.0, adsorption of the analyte on the MIP film decreased. One reason of the changes can be explained by the fact that acephate binds to the imprinted sites of the MIP film by hydrogen bonds. Based on the pK_a values (4.9 and 5.5) of MAA and polymeric MAA [41,42], we infer that 5 of the pH value approaches to the iso-electric point of the imprinted polymer film. The carboxyl group on the imprinted sites is the free form at pH 5.0, the hydrogen of the amino group and the oxygen of the carbonyl of the acephate form a cooperative ringed hydrogen bond with the carboxyl group of MAA. As the result, high affinity and selectivity of the MIP film toward acephate are achieved. This results in stronger hydrogen-binding interactions between acephate and the MIP film. Acephate in the aqueous solution is protonized while pH is less than 5, and the carboxyl group on the imprinted sites is ionized when pH is more than 5. Both cases can weaken the cooperative hydrogen-binding interaction between acephate and the MIP film. Another possibility of pH-optimum is a more compact film with more interaction sites on the SPR sensor chip. For the polymer film, the SPR signal will show decreasing binding concentration with a more swelled polymer. At the iso-electric point of the polymer (pH 5.0), it is expected to be more compact than outside the iso-electric point and the imprinted sites can be provided with good complementarity to the template in size, shape and position of functional groups. Hence, pH of the tested solutions was adjusted to 5.0 for all of the experiments.

3.3. Effect of molecular imprinting on FT-SPR sensor sensitivity

The MIP film was compared to the NIP film as a sensing material. Both sensor chips were prepared and treated in an identical manner. The effect of various concentrations of acephate on the SPR reflectivity minimum wavenumber shift on the acephate-imprinted polymer film and the NIP film was showed

Table 2
Analytical results of acephate for the apple and cole samples prepared in the first way ($n = 9$).

Samples	Found level without addition of acephate (mol/kg)	Spiked level (mol/kg)	Found level (mol/kg)	Recovery (%)	RSD (%)
Apple	0.00	2.00×10^{-11}	1.96×10^{-11}	98.0	1.9
Cole	0.00	5.00×10^{-12}	4.83×10^{-12}	96.6	1.4

in Fig. 3. The imprinted sensor chip exhibited a larger shift in SPR wavenumber compared to the non-imprinted blank chip. For the imprinted sensor chip, the SPR wavenumber change saturated above 2.0×10^{-11} M of acephate. Although the non-imprinted sensor chip also detected acephate, its sensitivity was significantly lower, resulting in smaller changes in SPR wavenumber with an increase of acephate concentration.

In Fig. 3, we still found that the plot of the resonance wavenumber shift versus acephate concentration showed a very good linearity in the acephate concentration range from 0.5×10^{-12} to 8.0×10^{-12} M (Fig. 3 inset) ($R^2 = 0.9998$). However, for the NIP film, the calibration curve has a poorer linearity and lower sensitivity. This resulted from low nonspecific affinity of the non-imprinted sensor chip to acephate. This result strongly suggests that molecular imprinting is effective for enhancing the acephate sensitivity of the sensor chip. It should explain that, there are the specific sites resulted from molecular imprinting and the nonspecific sites because of excess of the functional monomer MAA for the MIP film. It is well known that affinity of the specific sites for the template is much more than that of the nonspecific sites. In the low template concentration range, the specific binding of the MIP film for the template is preferential, and a very good linearity for the binding of the MIP film to the template occurs. With increasing template concentration, the binding of the specific sites is saturated and simultaneously the nonspecific binding appears. So both different types of binding sites result in the unquantifiable relation between acephate concentration and the binding sites in the acephate concentration range of 8.0×10^{-12} to 2.0×10^{-11} M. In the MIP film, monomer molecules (MAA) assemble around a molecular template (acephate) and become immobilized by cross-linking, forming a tailor-made binding site for the molecular template. The binding of acephate to the binding sites in the MIP film can be described by the Langmuir isotherm model [43]. According to this model,

$$K_{ass} = \frac{\theta}{(\alpha - \theta)[\text{acephate}]} \quad (1)$$

where θ is the number of sites occupied by acephate, and α is the total number of binding sites. At any given bulk concentration of acephate, the value of θ can be evaluated by Eq. (1). From the Langmuir equation, the Lineweaver–Burk relation is yielded.

$$\frac{1}{\theta} = \frac{1}{\alpha} + \frac{1}{\alpha K_{ass}}[\text{acephate}] \quad (2)$$

From the ratio of the slope and intercept, the values of K_{ass} can be obtained. Assuming that the wavenumber shift is proportional to the number of acephate-occupied sites, we analyzed the curve for the MIP film in Fig. 3 and an equation of the Langmiur isotherm was obtained to be $1/\theta = 0.06198 + 8.04867 \times 10^{-15}$ [acephate]. The association constant for the imprinted sites (K_{ass}) was calculated to be 7.7×10^{12} M^{-1}.

3.4. Selectivity of the MIP-coated sensor chip

To evaluate the cross-selectivity of the imprinted film, the changes in the resonance wavenumber of acephate were compared to those of other structurally related analogues (Fig. 4), such as malathion, phoxim, chlorpyrifos, methamidophos, profenofos and trichlorfor. Fig. 4 summarized the relative SPR wavenumber shifts upon addition of the OPPs. As shown in Fig. 4, acephate resulted in the largest response among the tested OPPs on the imprinted sensor chip. For the MIP-Au film, selectivity efficiency is defined by the following equation:

$$\text{Selectivity efficiency} = \frac{\Delta R_{\text{analogues}}}{\Delta R_{\text{acephate}}} \quad (3)$$

Here, ΔR is the difference of SPR wavenumber shifts upon addition of the OPPs. According to Eq. (3), the selectivity efficiencies of acephate, methamidophos, trichlorfor, phoxim, malathion, chlorpyrifos and profenofos were calculated to be 1.0, 0.37, 0.13, 0.18, 0.22, 0.17 and 0.11, respectively. These results imply that the MIP film exhibits high selectivity for acephate. But the non-imprinted sensor chip exhibited the smallest response to the tested OPPs. Interestingly, the order of the SPR wavenuber shifts on the non-imprinted sensor chip roughly depended on molecular weight: OPPs with a higher molecular weight caused a larger response. The imprinting of acephate in the MIP film is facilitated by the formation of hydrogen bonds between the functional groups of acephate and the carboxyl group in MAA. For other OPPs tested, the imprinted sensor chip has little higher selectivity. This suggests that the other OPPs tested are partially specific to the binding sites created by acephate.

3.5. Evaluation of the method

To demonstrate the applicability of the coupled MIP-SPR method for the analysis of real samples, apple and cole samples were spiked with acephate by two different ways. Based on Fig. 3 (inset), acephate contents in the samples were estimated by the proposed FT-SPR method. The original apple and cole samples without the addition of acephate were also determined to test whether the real samples contained acephate residue. Table 2 indicated that the recovery and precision of the method was evaluated by nine replicated measurements of apple (cole) spiked with acephate standards at a concentration of 2.00×10^{-11} (5.00×10^{-12}) mol/kg. The recoveries were 98.0% for apple and 96.6% for cole. Based on a signal to noise ratio of 3, the detection limits are 1.14×10^{-13} M for apple and 4.29×10^{-14} M for cole. To further demonstrate the applicability of the proposed method for the determination of acephate in real samples, another kind of synthetic samples were prepared. The total amount of absorbed acephate by the samples and the residue in dipped solution was determined. The total recoveries were shown in Table 3. The results show that this method has good reproducibility and highly sensitive and

Table 3
Analytical results of acephate for the apple and cole samples prepared in the second way ($n = 9$).

Samples	Content in original dipped solution (mol)	Found level in samples (mol)	Residual content in dipped solution (mol)	Recovery %)	RSD (%)
Apple (10 g)	3.0×10^{-11}	1.24×10^{-11}	1.74×10^{-11}	99.6	4.2
Cole (20 g)	3.0×10^{-11}	1.48×10^{-11}	1.49×10^{-11}	99.0	4.7

selective for the analysis of acephate in comparison with other methods [5,44,45].

4. Conclusion

An ultrathin film was prepared on Au surfaces by a surface-bound photo-radical initiator for a surface plasmon resonance (SPR) sensor detection of an aqueous acephate. We found that the association constant of acephate to the imprinted sites of the matrix is $7.7 \times 10^{12}\ M^{-1}$. The MIP ultrathin film exhibited a linear response in the range of 0.5×10^{-12}–8.0×10^{-12} M ($R^2 = 0.9998$) for the detection of acephate. The selectivity efficiencies of acephate and other structurally related analogues indicated the strong binding affinity for acephate. The results from two different kinds of samples demonstrate that the MIP-SPR system has great capability for providing highly selective analysis of organophosphate pesticides, suggesting that a combination of SPR sensing with MIP ultrathin film is a promising alternative method for the detection of acephate.

Acknowledgements

This work has been funded by National High-tech RD Program (863 program, No. 2007AA10Z432) and the National Natural Science Foundation of China (No. 30871756).

References

[1] C.D.S. TomLin (Ed.), The Pesticide Manual, 11th ed., British Crop Protection Council, Surrey, 1997.
[2] C.M. Torres, Y. Pico, J. Manes, J. Chromatogr. A 754 (1996) 301–331.
[3] P. Lea, F. Mladen, Biosens. Bioelectron. 18 (2003) 1–9.
[4] M. Natangelo, S. Tavazzi, R. Fanelli, E. Benfenati, J. Chromatogr. A 859 (1999) 193–201.
[5] A. Garrido Frenich, M.J. González-Rodríguez, F.J. Arrebola, J.L. Martínez Vidal, Anal. Chem. 77 (2005) 4640–4648.
[6] A. Cappiello, G. Famiglini, P. Palma, F. Mangani, Anal. Chem. 74 (2002) 3547–3554.
[7] M.A. Rodríguez-Delgado, J. Hernández-Borges, J. Sep. Sci. 30 (2007) 8–14.
[8] J.W. Wong, M.K. Hennessy, D.G. Hayward, A.J. Krynitsky, I. Cassias, F.J. Schenck, J. Agric. Food Chem. 55 (2007) 1117–1128.
[9] L. Lea Pallaroni, C. von Holst, J. Chromatogr., A 993 (2003) 39–45.
[10] R. Krska, S. Baumgartner, R. Josephs, Fresenius J. Anal. Chem. 371 (2001) 285–299.
[11] Z.L. Xu, G.M. Xie, Y.X. Li, B.F. Wang, R.C. Beier, H.T. Lei, H. Wang, Y.D. Shen, Y.M. Sun, Anal. Chim. Acta 647 (2009) 90–96.
[12] J.Y. Shim, Y.A. Kim, E.H. Lee, Y.T. Lee, H.S. Lee, J. Agric. Food Chem. 56 (2008) 11551–11559.
[13] M.A. Taipa, Comb. Chem. High Throughput Screen 11 (2008) 325–335.
[14] B. Liedberg, C. Nylander, I. Lundstrom, Sens. Actuators B (1983) 299–305.
[15] P.B. Daniels, J.K. Deacon, M.J. Eddowes, D.G. Pedley, Sens. Actuators 15 (1988) 11–18.
[16] H. Raether, Springer Tracts in Modern Physics;, vol. 111, Springer-Verlag, Berlin, Heidelberg, 1988.
[17] W. Knoll, Annu. Rev. Phys. Chem. 49 (1998) 569–638.
[18] E.A. Smith, M. Kyo, H. Kumasawa, K. Nakatani, I. Saito, R.M. Corn, J. Am. Chem. Soc. 124 (2002) 6810–6811.
[19] M. Kyo, T. Yamamoto, H. Motohashi, T. Kamiya, T. Kuroita, T. Tanaka, J.D. Engel, B. Kawakami, M. Yamamoto, Genes Cells 9 (2004) 153–164.
[20] M. Piliarik, H. Vaisocherova, J. Homola, Biosens. Bioelectron. 20 (2005) 2104–2110.
[21] H.J. Lee, Y. Yan, G. Marriott, R.M. Corn, J. Physiol. 563 (2005) 61–71.
[22] G. Metz, H. Ottlesen, D. Vetter, in: H.J. Bohm, G. Schneider (Eds.), Protein-Ligand Interactions: From Molecular Recognition to Drug Design, 2003, Weinheim, Wiley-VCH, 2003, pp. 213–236.
[23] D. Vetter, J. Cell. Biochem. (Suppl. 39) (2002) 79–84.
[24] J.M. McDonnell, Curr. Opin. Chem. Biol. 5 (2001) 572–577.
[25] R.M. Corn, S.C. Weibel, in: J. Chalmers, P. Griffiths (Eds.), Handbook of Vibrational Spectroscopy., vol. 2, Wiley, New York, 2002, pp. 1057–1064.
[26] G. Wulff, Ann. N.Y. Acad. Sci. 434 (1984) 327–333.
[27] K. Haupt, Anal. Chem. 75 (2003) 376A–383A.
[28] L.Q. Lin, J. Zhang, Q. Fu, L.C. He, Y.C. Li, Anal. Chim. Acta 561 (2006) 178–182.
[29] J.O. Mahony, K. Nolan, M.R. Smyth, B. Mizaikoff, Anal. Chim. Acta 534 (2006) 31–39.
[30] L.K. Ista, S. Mendez, V.H. Pérez-Luna, G.P. López, Lagmuir 17 (2001) 2552–2555.
[31] K. Haupt, N. Krzysztof, K. Wlodzimierz, Anal. Commun. 36 (1999) 391–393.
[32] A. Kugimiya, T. Takeuchi, Biosens. Bioelectron. 16 (2001) 1059–1062.
[33] C.J. Percival, S. Stanley, M. Galle, A. Braithwaite, M.I. Newton, G. McHale, W. Hayes, Anal. Chem. 73 (2001) 4225–4228.
[34] T. Panasyuk-Delaney, V.M. Mirsky, O.S. Wolfbeis, Electroanalysis 14 (2002) 221–224.
[35] O.A. Raitman, V.I. Chegel, A.B. Kharitonov, M. Zayats, E. Katz, I. Willner, Anal. Chim. Acta 504 (2004) 101–111.
[36] M. Lotierzo, O.Y.F. Henry, S. Piletsky, I. Tothill, D. Cullen, M. Kania, B. Hock, A.F.P. Turner, Biosens. Bioelectron. 20 (2004) 145–152.
[37] T. Piacham, Å. Josell, H. Arwin, V. Prachayasittikul, L. Ye, Anal. Chim. Acta 536 (2005) 191–196.
[38] D. Spivak, M.A. Gilmore, K.J. Shea, J. Am. Chem. Soc. 119 (1997) 4388–4393.
[39] F. Lanza, A.J. Hall, B. Sellergren, A. Bereczki, G. Horvai, S. Bayoudh, P.A.G. Cormack, D.C. Sherrington, Anal. Chim. Acta 435 (2001) 91–106.
[40] F. Puoci, G. Cirillo, M. Curcio, F. Iemma, U.G. Spizzirri, N. Picci, Anal. Chim. Acta 593 (2007) 164–170.
[41] N.A. Peppas, K.M. Wood, J.O. Blanchette, Expert Opin. Biol. Ther. 4 (2004) 881–887.
[42] J. Zhang, N.A. Peppas, Macromolecules 33 (2000) 102–107.
[43] R. Mazel, Principles of Adsorption and Reaction on Solid Surfaces, vol. 240, Wiley Interscience, New York, 1996.
[44] H.G.J. Mol, R.C.J. van Dam, O.M. Steijger, J. Chromatogr., A 1015 (2003) 119–127.
[45] K. Banerjee, D.P. Oulkar, S.B. Patil, M.R. Jadhav, S. Dasgupta, S.H. Patil, S. Bal, P.G. Adsule, J. Agric. Food Chem. 57 (2009) 4068–4078.